

Mark L. Brongersma
Pieter G. Kik
Editors

SPRINGER SERIES IN OPTICAL SCIENCES

Surface Plasmon Nanophotonics

 Springer

Brongersma

Kik

Editors

Surface Plasmon Nanophotonics

The development of advanced dielectric photonic structures has enabled tremendous control over the propagation and manipulation of light. Structures such as waveguides, splitters, mixers, and resonators now play a central role in the telecommunications industry. This book will discuss an exciting new class of photonic devices, known as surface plasmon nanophotonic structures. Surface plasmons are easily accessible excitations in metals and semiconductors and involve a collective motion of the conduction electrons. These excitations can be exploited to manipulate electromagnetic waves at optical frequencies ("light") in new ways that are unthinkable in conventional dielectric structures. The field of plasmon nanophotonics is rapidly developing and impacting a wide range of areas including: electronics, photonics, chemistry, biology, and medicine. The book will highlight several exciting new discoveries that have been made, while providing a clear discussion of the underlying physics, the nanofabrication issues, and the materials considerations involved in designing plasmonic devices with new functionality.

Surface Plasmon Nanophotonics is aimed to researchers and students interested in entering the field of plasmon nanophotonics, while serving as a reference to scientists already active in this area of research. It is written at the level of a first year graduate student with some background in electromagnetic theory and working knowledge of Maxwell's equations.

ISBN 978-1-4020-4349-9



Springer Series in

OPTICAL SCIENCES

The Springer Series in Optical Sciences, under the leadership of Editor-in-Chief *William T. Rhodes*, Georgia Institute of Technology, USA, provides an expanding selection of research monographs in all major areas of optics: lasers and quantum optics, ultrafast phenomena, optical spectroscopy techniques, optoelectronics, quantum information, information optics, applied laser technology, industrial applications, and other topics of contemporary interest.

With this broad coverage of topics, the series is of use to all research scientists and engineers who need up-to-date reference books.

The editors encourage prospective authors to correspond with them in advance of submitting a manuscript. Submission of manuscripts should be made to the Editor-in-Chief or one of the Editors. See also www.springeronline.com/series/624

Editor-in-Chief

William T. Rhodes

Georgia Institute of Technology
School of Electrical and Computer Engineering
Atlanta, GA 30332-0250, USA
E-mail: bill.rhodes@ece.gatech.edu

Editorial Board

Ali Adibi

Georgia Institute of Technology
School of Electrical and Computer Engineering
Atlanta, GA 30332-0250, USA
E-mail: adibi@ee.gatech.edu

Toshimitsu Asakura

Hokkai-Gakuen University
Faculty of Engineering
1-1, Minami-26, Nishi 11, Chuo-ku
Sapporo, Hokkaido 064-0926, Japan
E-mail: asakura@eli.hokkai-s-u.ac.jp

Theodor W. Hänsch

Max-planck-Institut für Quantenoptik
Hans-Kopfermann-Straße 1
85748 Garching, Germany
Email: t.w.haensch@physik.uni-muenchen.de

Takeshi Kamiya

Ministry of Education, Culture, Sports
Science and Technology
National Institution for Academic Degrees
3-29-1 Otsuka, Bunkyo-ku
Tokyo 112-0012, Japan
E-mail: kamiyatk@niad.ac.jp

Ferenc Krausz

Ludwig-Maximilians-Universität München
Lehrstuhl für Experimentelle Physik
Am Coulombwall 1
85748 Garching, Germany
and
Max-Planck-Institut für Quantenoptik
Hans-Kopfermann-Straße 1

85748 Garching, Germany

E-mail: ferenc.krausz@mpq.mpg.de

Bo Monemar

Department of Physics
and Measurement Technology
Materials Science Division
Linköping University
58183 Linköping, Sweden
E-mail: bom@ifm.liu.se

Motoichi Ohtsu

University of Tokyo
Department of Electronic Engineering
7-3-1 Hongo, Bunkyo-ku
Tokyo 113-8959, Japan
E-mail: ohtsu@ee.t.u-tokyo.ac.jp

Herbert Venghaus

Fraunhofer Institut für Nachrichtentechnik
Heinrich-Hertz-Institut
Einsteinufer 37
10587 Berlin, Germany
E-mail: venghaus@hhi.de

Horst Weber

Technische Universität Berlin
Optisches Institut
Straße des 17. Juni 135
10623 Berlin, Germany
E-mail: weber@physik.tu-berlin.de

Harald Weinfurter

Ludwig-Maximilians-Universität München
Sektion Physik
Schellingstraße 4/III
80799 München, Germany
E-mail: harald.weinfurter@physik.uni-muenchen.de

Mark L. Brongersma Pieter G. Kik
(Editors)

Surface Plasmon Nanophotonics

With 147 Figures

 Springer

A C.I.P. Catalogue record for this book is available from the Library of Congress.

ISBN: 978-1-4020-4349-9 (HB)
ISBN: 978-1-4020-4333-8 (e-book)

Published by Springer,
P.O. Box 17, 3300 AA Dordrecht, The Netherlands.

www.springer.com

Printed on acid-free paper

All rights reserved.
© 2007 Springer

No part of this work may be reproduced, stored in a retrieval system, or transmitted in any form or by any means, electronic, mechanical, photocopying, microfilming, recording or otherwise, without written permission from the Publisher, with the exception of any material supplied specifically for the purpose of being entered and executed on a computer system, for exclusive use by the purchaser of the work.

CONTENTS

Preface	vii
1. Surface Plasmon Nanophotonics <i>Pieter G. Kik and Mark L. Brongersma</i>	1
2. Near-Field and Far-Field Properties of Nanoparticle Arrays <i>Andreas Hohenau, Alfred Leitner and Franz R. Aussenegg</i>	11
3. Theory of Light Transmission Through Periodically Structured Nano-Apertures <i>F.J. García-Vidal, F. López-Tejiera, J. Bravo-Abad and L. Martín-Moreno</i>	27
4. Development and Near-Field Characterization of Surface Plasmon Waveguides <i>J.-C. Weeber, A.-L. Baudrion, M. U. González, A. Dereux, Rashid Zia and Mark L. Brongersma</i>	39
5. Numerical Simulations of Long-Range Plasmonic Transmission Lines <i>Aloyse Degiron and David R. Smith</i>	55
6. Surface Plasmon Polariton Guiding in Photonic Bandgap Structures <i>Thomas Søndergaard and Sergey I. Bozhevolnyi</i>	73
7. Subwavelength-Scale Plasmon Waveguides <i>Harry A. Atwater, Jennifer A. Dionne and Luke A. Sweatlock</i>	87
8. Optical Superlens <i>X. Zhang, M. Ambati, N. Fang, H. Lee, Z. Liu, C. Sun and Y. Xiong</i>	105
9. Optical Field Enhancement with Plasmon Resonant Bowtie Nanoantennas <i>G.S. Kino, Arvind Sundaramurthy, P.J. Schuck, D.P. Fromm and W.E. Moerner</i>	125

10. Near-Field Optical Excitation and Detection of Surface Plasmons <i>Alexandre Bouhelier and Lukas Novotny</i>	139
11. Principles of Near-Field Optical Mapping <i>Alain Dereux</i>	155
12. Overview of Simulation Techniques for Plasmonic Devices <i>Georgios Veronis and Shanhui Fan</i>	169
13. Plasmon Hybridization in Complex Nanostructures <i>J.M. Steele, N.K. Grady, P. Nordlander and N.J. Halas</i>	183
14. Sensing Proteins with Adaptive Metal Nanostructures <i>Vladimir P. Drachev, Mark D. Thoreson and Vladimir M. Shalaev</i>	197
15. Integrated Optics Based on Long-Range Surface Plasmon Polaritons <i>Pierre Berini</i>	217
16. Localized Surface Plasmons for Optical Data Storage Beyond the Diffraction Limit <i>Junji Tominaga</i>	235
17. Surface Plasmon Coupled Emission <i>Zygmunt Gryczynski, Evgenia G. Matveeva, Nils Calander, Jian Zhang, Joseph R. Lakowicz and Ignacy Gryczynski</i>	247
Index	267

PREFACE

At the moment the first issue of this book appears, hundreds of groups around the world are pushing the boundaries of the field of surface plasmon nanophotonics. The newfound ability to use metallic nanostructures to manipulate light at a length scale far below the diffraction limit has opened a myriad of exciting opportunities. Based on the exponential increase in the number of published papers every year (Chapter 1), it is clear that we are at the eve of a new revolution that will impact many fields of science and technology, including photonics, computation, the Internet, biology, medicine, materials science, physics, chemistry, and photovoltaics.

It has been a great pleasure and honor to work with some of the leading scientists in the field during the preparation of this work. The book truly reflects the present status of this rapidly developing area of science and technology and highlights some of the important historic developments. Most of the chapters discuss ongoing scientific research, and promising future directions are identified. Plasmon excitations in single and periodic arrays of metallic nanostructures are discussed in Chapters 2 and 3. The unique properties of metallic waveguides and metallo-dielectric photonic crystal structures that can route information on a chip are treated in Chapters 3 through 7. Surface Plasmon Mediated Field Concentration and Imaging methods, including superlenses and nanoscale optical antennas, are described in Chapters 8 through 10. The rapid developments in nanoscale optical probes that can visualize the flow of light and new, powerful electromagnetic simulation tools are treated in Chapters 11 through 13. The final chapters (Chapters 14–17) analyze a set of exciting applications of surface plasmon nanophotonics with tremendous commercialization potential, ranging from biology to data storage, and integrated optics.

We would like to thank all of the contributing authors for providing us with such excellent snapshots of the current state of the field of plasmonics. We would also like to acknowledge Kathleen Di Zio and Beatriz Roldán Cuenya for boundless mental and moral support. Kathy also contributed in a significant way by carefully proofreading many of the chapters and providing useful editorial comments. It has been a great pleasure to work with each and every one of you.

The Editors
Mark L. Brongersma
Pieter G. Kik

CHAPTER THREE

THEORY OF LIGHT TRANSMISSION THROUGH PERIODICALLY STRUCTURED NANO-APERTURES

F.J. GARCÍA-VIDAL¹, F. LÓPEZ-TEJEIRA², J. BRAVO-ABAD¹ AND L. MARTÍN-MORENO²

¹Departamento de Física Teórica de la Materia Condensada, Universidad Autónoma de Madrid, E-28049, Spain

²Departamento de Física, de la Materia Condensada, ICMA-CSIC, Universidad de Zaragoza, E-50009 Zaragoza, Spain

3.1. INTRODUCTION

As illustrated throughout this book, surface plasmons (SPs) are well known for their capabilities of concentrating light in subwavelength volumes and also for guiding light along the surface of a metal. But this does not exhaust the phenomena related to SPs. Even the scientific community working on this subject was greatly surprised in 1998 by the suggestion that SPs could enhance the transmission of light through subwavelength holes.¹ That seminal paper reported that, when subwavelength holes are disposed on a metallic film forming a two-dimensional (2D) array, the transmission of light through this structure is greatly enhanced at some particular wavelengths. The locations of the transmission peaks appearing in the experimental spectra could be approximately found from the dispersion relation of SPs modes running on the metal surface. Then, from the beginning of the history of this subject, it was clear that there was a close connection between extraordinary optical transmission (EOT) and the excitation of SPs. Since 1998, several experimental and theoretical groups around the world have reproduced the main features found in the first set of experiments. The dependence of this phenomenon with the type of metal (noble metals show larger enhancements), type of lattice (square or triangular), shape of the holes (circular, elliptical, square or rectangular) and frequency regime (optical, THz or microwave) have been thoroughly analyzed.^{2–13} Four years after the discovery of EOT in 2D hole arrays, it was also reported¹⁴ that EOT phenomenon also appears in a single aperture (hole or slit) flanked by periodic corrugations in the side of the metal film the light is impinging on. Moreover, it was also found that very strong directional emission

(beaming) is possible through single apertures if the corrugation is placed on the exit side. In this chapter, we concentrate on the explanation of the fundamental physics behind the phenomenon of EOT both in 2D hole arrays and in single apertures and also behind the beaming effect observed in single apertures surrounded by periodic corrugations.

3.2. TWO-DIMENSIONAL SUBWAVELENGTH HOLE ARRAYS

Our goal in this section is to explain the physical origin of EOT in subwavelength hole arrays.

Let us briefly describe the basic ingredients of our theoretical formalism that was presented in Ref. 3 for the case of a 2D array of square holes and in Ref. 15 for circular holes. In our formalism, the dielectric constant of the metal is taken into account by considering surface impedance boundary conditions¹⁶ (SIBC) on the metal-interfaces defining the metal film. However, in the metal walls defining the hole, the metal is treated as a perfect conductor. This approximation greatly simplifies the formalism as it allows the expression of the electromagnetic (EM) wavefield inside the hole in terms of the eigenmodes of the hole. For simple hole shapes (such as rectangular, triangular or circular), these eigenmodes are known analytically.¹⁷ This approximation, therefore, neglects absorption by the metal walls surrounding the hole. It is expected that this approach is not too bad as the area of the “horizontal” metal-dielectric interfaces (in which absorption is properly taken into account) is much larger than the “vertical” ones, for the geometrical parameters typically analyzed in the experiments. However, assuming perfect conductor walls also neglects the penetration of the EM fields. This is an important deficiency, as it is well known that in the optical regime EM fields penetrate into the metal up to a distance mainly controlled by the skin depth of the metal (of the order of 10–20 nm for noble metals). We circumvent this deficiency by considering an (wavelength dependent) effective hole radius such that the propagation constant inside the hole is equal to the one extracted from an exact calculation. Within these approximations, the calculation of the transmission properties of 2D hole arrays amounts to expanding the EM fields in terms of the Bloch EM modes in each spatial region (plane waves in vacuum regions and hole waveguide modes inside the holes), and obtaining the expansion coefficients by just matching appropriately the parallel components of the E- and H-fields in the two metal-dielectric interfaces.

In Fig. 3.1 we plot the result of our numerical simulation corresponding to the geometrical values of the structure experimentally analyzed in Fig. 1 of Ref. 3, but this time the calculation considers circular holes. Clearly, our model is capturing the main features of the experimental spectrum; the position of the highest peak (located at around 780 nm) is in reasonable agreement with the experimental data. However, the experimental peak is lower and wider than the one obtained in the calculations. This could be indicative of the presence of disorder and/or finite size effects.

In order to gain physical insight into this phenomenon, it is important to look for the minimal model in which EOT is still present. In Fig. 3.2 we compare the result of the fully converged calculation (solid curve) displayed in Fig. 3.1 with the one

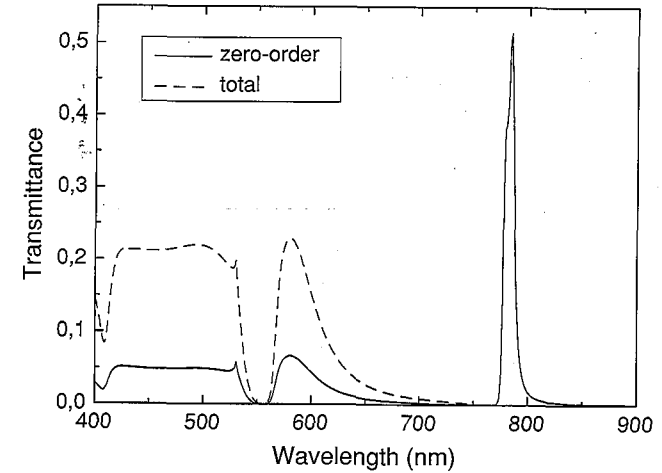


Figure 3.1. Zero-order transmittance (solid curve) and total transmittance (dashed curve) calculated for a 2D hole array (period of the array, $d = 750$ nm and the diameter of the circular holes, $a = 280$ nm) perforated in a silver film of thickness $h = 320$ nm.

(dashed curve) obtained by just considering one eigenmode inside the hole (the TE_{11} mode, the least decaying evanescent mode). As clearly seen in the figure, the inclusion of more evanescent modes inside the hole provokes a very small shift (2 nm) in the transmission peaks to shorter wavelengths but the overall picture of the spectrum

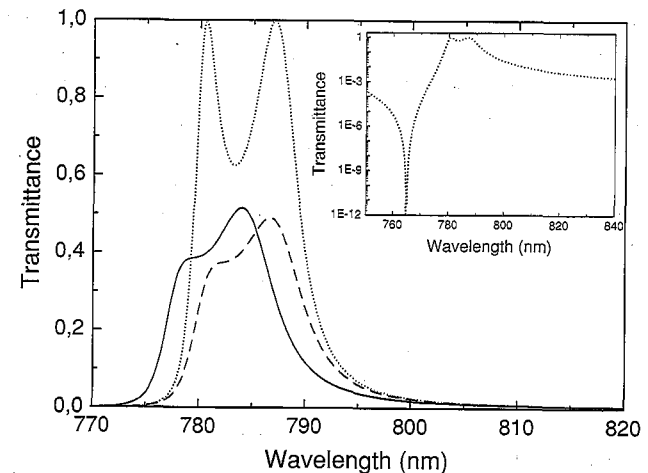


Figure 3.2. Zero-order transmittance for the structure analyzed in Fig. 3.1 obtained by using a fully converged calculation (solid curve), by only considering the TE_{11} mode inside the holes (dashed curve) and the same calculation as the dashed curve but assuming that no absorption is present in the metal (dotted curve); this case is also displayed in the inset but in a logarithmic scale.

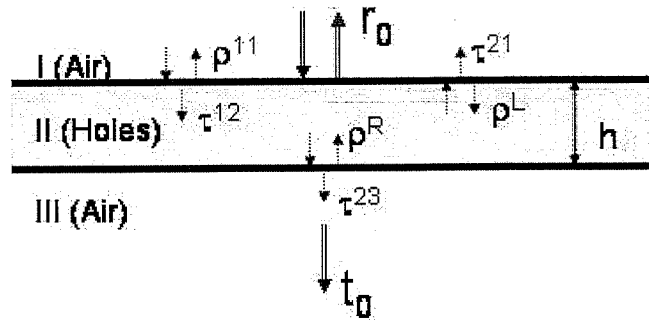


Figure 3.3. Schematic drawing of the different scattering magnitudes at interfaces I–II and II–III. See text for a detailed explanation of the different terms.

remains the same. Moreover, by neglecting the absorption in the metal film (in our calculations we can do it very easily by assuming that the imaginary part of the dielectric constant of silver is zero), we find that the spectrum has two peaks (dotted curve) that reach 100% transmittance and that the net effect of the absorption in the metal is to reduce the amount of light emerging from the structure without altering the physical picture. In the inset of the figure, we plot this last curve in logarithmic scale in order to better illustrate the presence of a zero (the so-called Wood's anomaly, see Ref. 1) in the transmittance spectrum. We will discuss the origin of this zero later on.

From now on in this section we are going to analyze the results of this minimal model (only TE_{11} considered and $\text{Im}(\varepsilon(\omega)) = 0$). In order to unveil the physical mechanism responsible for EOT and to relate EOT with the SPs modes of the metal-dielectric interfaces, we calculate the transmittance through the structure within the multiple scattering formalism. Within this framework, transmission amplitudes for crossing the whole system can be obtained from the scattering amplitudes for crossing the two different individual metal-dielectric interfaces and the propagation constant of the fundamental (TE_{11}) mode inside the hole (see Fig. 3.3).

The zero-order transmission amplitude (t_0) can be expressed then as:

$$t_0 = \frac{\tau_{12} e^{ik_z h} \tau_{23}}{1 - \rho^R \rho^L e^{2ik_z h}}, \quad (3.1)$$

where τ_{12} and τ_{23} are the transmission amplitudes for crossing the I–II and the II–III interfaces, respectively. $k_z = \sqrt{k_0^2 - (1,84/a)^2}$, k_0 is the EM wavenumber in vacuum, and ρ^R and ρ^L are the amplitudes for the TE_{11} mode to be reflected back into the hole at the II–III and II–I interfaces, respectively. In the symmetric system we are now considering where dielectric constants in reflection and transmission regions are equal, $\rho^R = \rho^L = g\rho$. In Fig. 3.4 we show the behavior of the modulus of τ_{12} , τ_{23} and ρ as a function of the wavelength for the case of a 2D square array with $d = 750$ nm of holes and $a = 280$ nm. There are several interesting features appearing in these scattering magnitudes. Firstly, the three quantities present a maximum at around

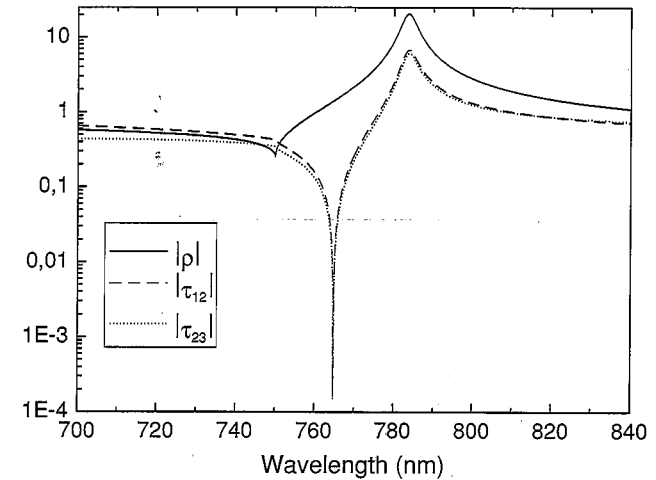


Figure 3.4. Modulus of ρ (solid), τ_{12} (dashed) and τ_{23} (dotted) as a function of the wavelength for a silver surface perforated with a 2D array of period $d = 750$ nm of circular holes with diameter $a = 280$ nm.

785 nm. Moreover, $|\rho| \gg 1$ at this resonant location. This counterintuitive result is due to the fact that the fundamental eigenmode inside the hole is evanescent, for which current conservation only restricts $\text{Im} \rho \geq 0$, with no restrictions applied to the real part of this scattering magnitude.

The strong peak in ρ (and in τ_{12} , and τ_{23}) signals the existence of a surface resonance (or surface leaky mode) of the perforated metal surface. Its spectral width is related to the time the EM field spends at the surface before it is either radiated or absorbed. This large reflection amplitude opens up the possibility of a resonant denominator in Eq. (3.1) even for metal thicknesses such that $e^{-2|k_z| h} \ll 1$.

Figure 3.5 illustrates graphically that the peaks appearing in the zero-order transmittance occur at the wavelengths for which the distance between $|\rho|$ and $e^{|k_z| h}$ is minimal. **This figure unambiguously shows that EOT in 2D hole arrays has a resonant nature and that the origin of this resonant behavior is the existence of SPs decorating the metal-dielectric interfaces.** For thin films ($h = 100 - 400$ nm in Fig. 3.5), the two curves intersect at two different wavelengths giving rise to the appearance of two transmission peaks in the spectrum. It can be shown that these two peaks correspond to the symmetric and antisymmetric combinations of the two SPs of the two interfaces that are coupled through the evanescent fields inside the holes. These two coupled surface modes are able to transfer energy very efficiently (100% if no absorption is present in the system) through the structure. When h is further increased, there is no crossing between the two curves and only one peak with associated transmittance less than 100% remains in the spectrum. As commented above, the location of this peak coincides with the location of the SP at parallel momentum $2\pi/d$ of the silver surface perforated with a 2D array of holes. A detailed discussion of the formation of the coupled surface modes and the typical times in the transmission process can be found in Ref. 3.

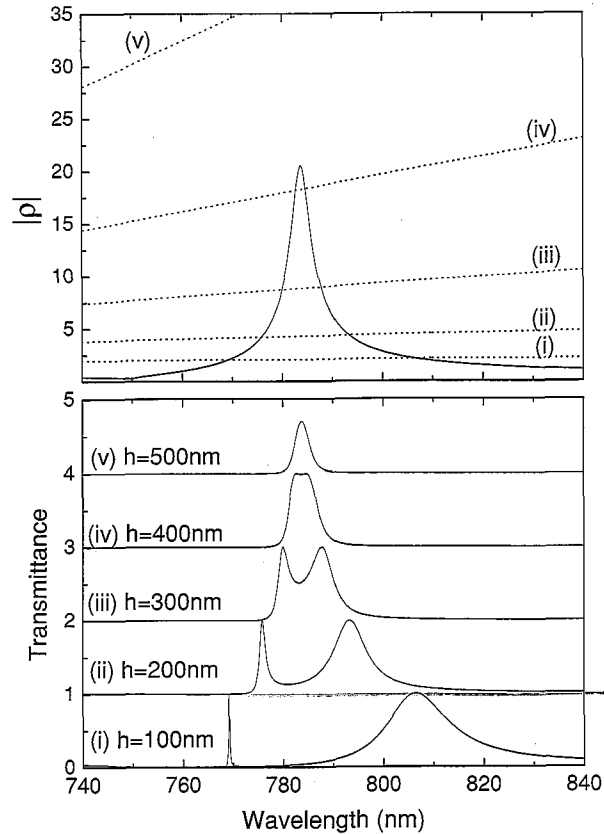


Figure 3.5. Upper panel: modulus of ρ and curves $\exp(|k_z|/h)$ for different values of h (100, 200, 300, 400 and 500 nm) for the same geometrical parameters than in the previous figures. Bottom panel: zero-order transmittance versus wavelength for the silver thicknesses considered in the upper panel.

An additional feature appearing in Fig. 3.4 is that both $|\tau_{12}|$ and $|\tau_{23}|$ have a zero located at around 765 nm, that translates into a minimum in the zero-order transmittance theoretical spectrum (see Fig. 3.2), the so-called Wood's anomaly. It is worth commenting that the location of this zero does not coincide with the location of the Rayleigh minimum that occurs when a propagating diffracted wave becomes evanescent (in this particular case this should appear at 750 nm). On the contrary, it can be shown that the location of the minima in both $|\tau_{12}|$ and $|\tau_{23}|$ coincides with the location of the SP at parallel momentum $2\pi/d$ of the **plain** (without holes) silver surface. This is the origin of some criticism on the relation of EOT and excitation of SPs.¹⁸ As we have stated here and already shown in Ref. 3, EOT is mediated by SPs but those corresponding to the structured metal surface.

Once EOT is explained in terms of the excitation of SPs in the optical regime, the question about the transferability of EOT to other frequency regimes naturally

arises. In Ref. 3 we showed that the EOT phenomenon also appears even in a perfect conductor film perforated with a 2D array of holes. A more extensive theoretical analysis of the existence of EOT in perfect conductors can be found in Ref. 15. But, flat perfect conductor interfaces do not possess SP modes. This could imply that the origins of EOT for metals in the optical regime and for perfect conductors are different. Importantly, surface EM modes appear in **corrugated** perfect conductors and, in particular, in perfect conductors perforated with 2D hole arrays. Very recently, we have shown that these surface EM modes are responsible for the existence of EOT in perfect conductors.¹⁹ Therefore, EOT seems to be a more general phenomenon that will appear in any electromagnetic structure in which surface EM modes are present and can couple to radiative modes. This hypothesis has been verified for metals in the THz¹² and microwave regimes¹³ and for photonic crystal waveguides.²⁰

3.3. EOT IN SINGLE APERTURES FLANKED BY CORRUGATIONS

As was discussed in the previous section, surface EM modes are at the origin of the EOT phenomenon. The two necessary ingredients for observing EOT are: (i) the existence of a surface EM mode and (ii) the presence of a grating coupler that allows the incident light to interact with the surface mode. Therefore, it was reasonable to expect that EOT phenomenon could also appear in a **single aperture** surrounded by a finite periodic array of indentations. This hypothesis was experimentally verified in Ref. 14 both for a 1D slit surrounded by a finite array of grooves and for a 2D circular hole flanked by circular trenches, the so-called *bull's eye* geometry. Here we present the theoretical foundation of this phenomenon for the 1D case.

We present a brief description of the theoretical formalism used to simulate the transmission of light through a single slit of width a symmetrically flanked by a finite array (with period d) of $2N$ grooves of width a and depth w (see Fig. 3.6). A normal incident p-polarized plane wave is impinging at the structure.

The theoretical formalism we have developed in order to describe the transmission properties of this type of structures is a non-trivial extension to finite structures of the framework previously used for analyzing 2D hole arrays. First we consider an artificial supercell with cell parameter L that includes the finite set of indentations we are

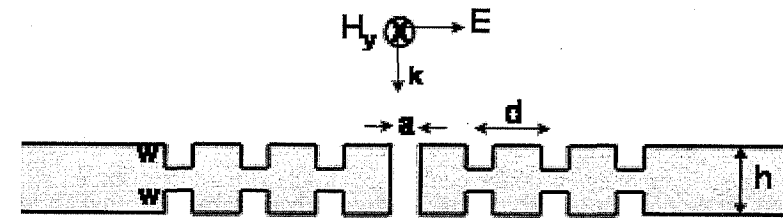


Figure 3.6. Schematic figure of the structure analyzed in this section: a single slit of width a , surrounded by grooves of width a and depth w in the input and output surfaces. The metal thickness is h and we analyze the transmission properties of this system for a normal incident p-polarized plane wave.

considering. Then we express the EM-fields in different regions in terms of their mode expansion. In vacuum we expand the fields by a set of plane waves whereas for the grooves and central slit only the fundamental propagating eigenmode is considered. That is, inside indentation α , E_x is a linear combination of $\phi_\alpha(x)e^{\pm ikz}$, where $2\pi/\lambda$ and $\phi_\alpha(x) = 1/\sqrt{a}$. Then we match the fields appropriately on all interfaces (as in the case of 2D hole arrays, in the horizontal interfaces we apply SIBC while perfect metal boundary conditions are assumed in the vertical ones). At the end the limit $L \rightarrow \infty$ is taken, leading to a set of linear equations for the unknowns $\{E_\alpha, E'_\gamma\}$:

$$\begin{aligned} [G_{\alpha\alpha} - \varepsilon_\alpha]E_\alpha + \sum_{\beta \neq \alpha} G_{\alpha\beta}E_\beta - \delta_{\alpha 0}G_V E'_\alpha &= I_\alpha \\ [G_{\gamma\gamma} - \varepsilon_\gamma]E'_\gamma + \sum_{\nu \neq \gamma} G_{\gamma\nu}E'_\nu - \delta_{\gamma 0}G_V E_\gamma &= 0 \end{aligned} \quad (3.2)$$

where α and γ runs over all indentations (slit or grooves). The set $\{E_\alpha\}$ gives the x -component of the electric field right at the indentations in the input surface: $E_x(z = 0^+) = \sum_\alpha E_\alpha \phi_\alpha(x)$ whereas the set $\{E'_\gamma\}$ describes the x -component of the electric field at the output surface: $E_x(z = h^-) = \sum_\gamma E'_\gamma \phi_\gamma(x)$. The different terms appearing in these *tight-binding* equations have a clear physical interpretation. I_α takes into account the direct initial illumination term over object α and it is basically the overlap integral between the incident p-polarized plane wave and wavefield ϕ_α . In this structure, the two metal interfaces are only connected through the central slit by the term $G_V = 1/\sin(kh) \cdot \varepsilon_\alpha$ measures the back-and-forth-bouncing of the EM fields inside indentation α : $\varepsilon_\alpha = \cot(kh)$ at the grooves ($\alpha \neq 0$) and $\varepsilon_0 = \cot(kh)$ for the slit. The term $G_{\alpha\beta}$ controls the EM coupling between indentations. It takes into account that each point in the indentation β emits radiation that can be collected by indentation α . Mathematically, $G_{\alpha\beta}$ is the projection onto wavefields ϕ_α and ϕ_β of the Green's function $G(\vec{r}, \vec{r}')$. It can be shown that this Green function contains the contribution of both diffraction modes and the SP channel. In general, it has to be computed numerically although in the case of perfect conductors its expression is known analytically as: $G = (i\pi/\lambda) H_0^{(1)}(k|\vec{r} - \vec{r}'|)$, $H_0^{(1)}$ being the 0-order Hankel function of the first kind. Once the values for $\{E_\alpha, E'_\gamma\}$ are calculated the normalized-to-area transmittance can be obtained from $T = G_V \text{Im}(E_0 E'_0)$.

In Fig. 3.7 we show the theoretical results for the normalized-to-area transmittance $T(\lambda)$ for a single slit surrounded by $2N$ grooves in the input side and located symmetrically (N to the left and right) with respect to the central slit. The set of geometrical parameters used is typical for experimental studies of this phenomenon in the optical regime ($a = 100$ nm, $d = 600$ nm, $w = 100$ nm and $h = 400$ nm).

The curve for $N = 0$ (solid curve) corresponds to the single slit case; in this frequency range, the spectrum presents two broad peaks that correspond to the excitation of slit waveguide modes inside the central slit.²¹ As the number of indentations increases, a maximum in $T(\lambda)$ develops at $\lambda_M = 755$ nm. For this set of geometrical values and for the metal considered, maximum in $T(\lambda)$ saturates at about $N = 5$ – 10 , when T is enhanced by a factor close to 5. With respect to the output corrugation, we have demonstrated in previous works (see Ref. 22) that it has little effect on the

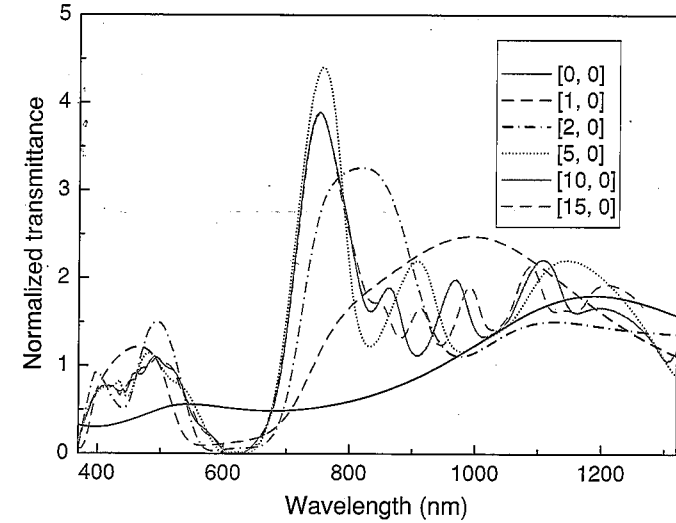


Figure 3.7. Normalized transmittance versus wavelength for a single slit of width $a = 100$ nm surrounded by $2N$ grooves (N ranging from 0 to 15) located symmetrically with respect to the central slit and only disposed in the input surface. In these calculations the output surface is not corrugated. The period of the array is $d = 600$ nm, the width of the grooves is also 100 nm and their depth is 100 nm. The silver film has a thickness of 400 nm.

total transmittance. From the set of Eqs. (3.2), it is possible to identify the different mechanisms that help to enhance the transmission of light through the central slit and are present in Fig. 3.7. The corresponding two equations for $\{E_0, E'_0\}$ are (assuming that the slit is flanked by the grooves only at the input surface):

$$\begin{aligned} [G_{00} - \varepsilon_0]E_0 + \sum_{\alpha \neq 0} G_{0\alpha}E_\alpha - G_V E'_0 &= I_0 \\ [G_{00} - \varepsilon_0]E'_0 - G_V E_0 &= 0 \end{aligned} \quad (3.3)$$

As commented before, one mechanism is already present in a single slit. For this particular case, $E_0 = 2(G_{00} - \varepsilon_0)/D$ and $E'_0 = 2G_V/D$ where the denominator $D = (G_{00} - \varepsilon_0)^2 - G_V^2$. For some particular wavelengths, D is very close to zero. These resonances are essentially slit waveguide modes. Corrugating the input surface opens up the possibility of having a large E_0 by having a large E_α . If we have a look to the equation for E_α , this magnitude can be large if $G_{\alpha\alpha} - \varepsilon_\alpha \approx 0$, that is the condition of the excitation of a groove cavity mode. However, in order to have a large E_0 , the illumination coming from the different grooves has to reach the central slit in phase. The phase in this re-illumination process is controlled by $G_{0\alpha}$. By looking at the asymptotic expression of $H_0^{(1)}(x) \approx e^{ikx}$, it is expected that all light re-emitted from the grooves reaches the other grooves and the central slit in phase for $\lambda \approx d$, although the presence of a SP channel in $G_{0\alpha}$ modifies slightly this condition as seen in Fig. 3.7. The combination of the two mechanisms described above (groove cavity mode and

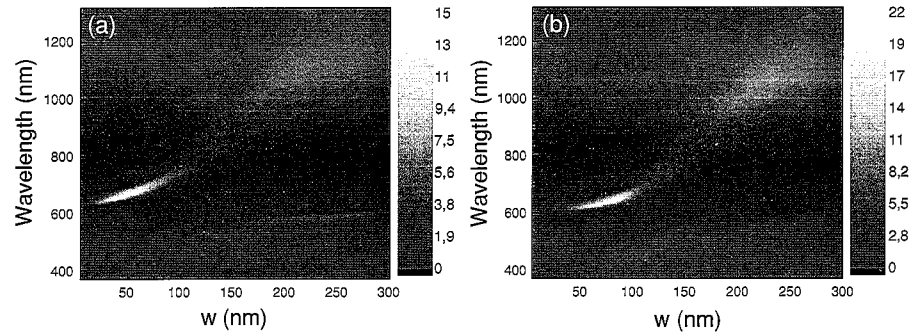


Figure 3.8. Normalized-to-area transmittance versus wavelength and depth of the grooves for a single slit of width 100 nm surrounded by 20 grooves located symmetrically in the input surface. The thickness of the metal film is 400 nm as in the previous figure. In panel (a), we are assuming SIBC in the horizontal interfaces of the structure whereas panel (b) shows the results for a perfect conductor film.

in-phase groove re-emission) is responsible for the peak located at around 755 nm appearing in Fig. 3.7.

In order to illustrate how the three different mechanisms influence the transmittance through the central slit, in Fig. 3.8(a) we show T versus λ and depth of the grooves, w , for $a = 100$ nm, $h = 400$ nm, $d = 600$ nm and $N = 10$. As clearly seen in this figure, when two mechanisms coincide, there is a boost in the transmittance. For small w , maximum transmittance appears close to the $\lambda \approx d$ condition. **It can be shown that this line corresponds to the excitation of a surface EM mode**, originated by the interplay between the groove cavity modes and the in-phase groove re-emission mechanisms. This surface mode has strong similarities with the one responsible for EOT in periodic apertures. It is quite interesting to compare the results we have presented in (a) with the ones obtained within the perfect conductor approximation and rendered in panel (b) of Fig. 3.8. The similarities between the results obtained in these two cases reinforces the conclusion that the main ingredients of the EOT phenomenon in 2D hole arrays and in single apertures is already present in corrugated perfect conductor surfaces.

3.4. BEAMING OF LIGHT IN SINGLE APERTURES

As commented before, it was found experimentally in Ref. 14 that the radiation pattern emerging from the structure (basically controlled by the output corrugation) presents a very small angular divergence at some resonant wavelengths. As a way of example, in Fig. 3.9 we show our calculated radial component of the Poynting vector, $S_r(\theta)$, in the far-field region and normalized to the total transmittance for a single slit surrounded symmetrically by $2N$ grooves in the output surface. The theoretical framework used is the same as the one described in previous section. Several N are presented (from 1 to 15) for the resonant wavelength $\lambda_M = 750$ nm.

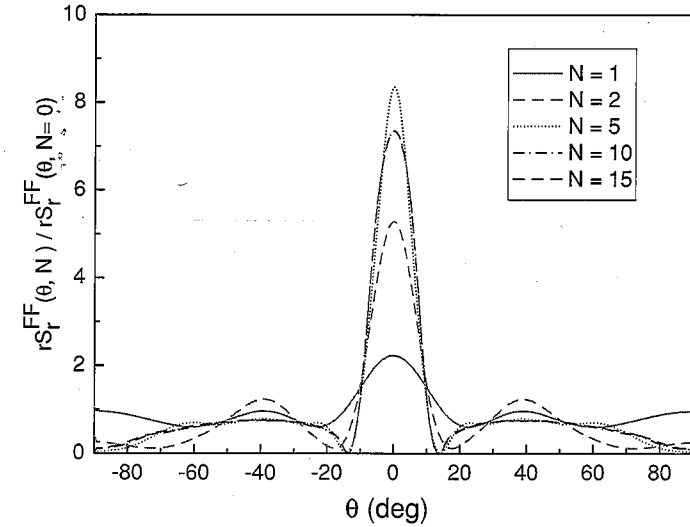


Figure 3.9. Radial component of the Poynting vector evaluated in the far field versus angle for a single slit of width $a = 100$ nm surrounded symmetrically by $2N$ grooves (N ranging from 1 to 15) of width 100 nm and depth 100 nm. The wavelength of the incident radiation is 750 nm.

Note that this resonant wavelength is the same as the one found for EOT in a single slit flanked by a finite array of grooves in the input surface for the same set of geometrical parameters. This fact clearly shows that the origin of the beaming effect is the same as the EOT in single apertures surrounded by periodic corrugations: the excitation of a surface EM mode in the output surface. Details about the formation of this surface mode and its relation with the radiation pattern mode can be found in Ref. 23.

REFERENCES

1. T.W. Ebbesen, H.J. Lezec, H.F. Ghaemi, T. Thio, P.A. Wolff: Extraordinary optical transmission through sub-wavelength hole arrays, *Nature* **391**(6668), 667–669 (1998).
2. H.F. Ghaemi, T. Thio, D.E. Grupp, T.W. Ebbesen, H.J. Lezec: Surface plasmons enhance optical transmission through subwavelength holes, *Phys. Rev. B* **58**(11), 6779–6782 (1998).
3. L. Martín-Moreno, F.J. García-Vidal, H.J. Lezec, K.M. Pellerin, T. Thio, J.B. Pendry, T.W. Ebbesen: Theory of extraordinary optical transmission through subwavelength hole arrays, *Phys. Rev. Lett.* **86**(6), 1114–1117 (2001).
4. L. Salomon, F.D. Grillot, A.V. Zayats, F. de Fornel, Near-field distribution of optical transmission of periodic subwavelength holes in a metal film, *Phys. Rev. Lett.* **86**(6), 1110–1113 (2001).
5. A. Krishnan, T. Thio, T.J. Kima, H.J. Lezec, T.W. Ebbesen, P.A. Wolff, J. Pendry, L. Martín-Moreno, F.J. García-Vidal: Evanescently coupled resonance in surface plasmon enhanced transmission, *Opt. Commun.* **200**(1–6), 1–7 (2001).
6. A. Degiron, H.J. Lezec, W.L. Barnes, T.W. Ebbesen: Effects of hole depth on enhanced light transmission through subwavelength hole arrays, *Appl. Phys. Lett.* **81**(23), 4327–4329 (2002).

7. N. Bonod, S. Enoch, L. Li, E. Popov, M. Nevière: Resonant optical transmission through thin metallic films with and without holes, *Opt. Exp.* **11**(5), 482–490 (2003).
8. C. Genet, M. P. van Exter, J.P. Woerdman: Fano type interpretation of red shifts and red tails in hole array transmission spectra, *Opt. Comm.* **225**(4–6), 331 (2003).
9. W.L. Barnes, W.A. Murray, J. Ditinger, E. Devaux, T.W. Ebbesen: Surface plasmon polaritons and their role in the enhanced transmission of light through periodic arrays of subwavelength holes in a metal film, *Phys. Rev. Lett.* **92**(10), 107401 (2004).
10. R. Gordon, A.G. Brolo, A. McKinnon, A. Rajora, B. Leathem, K.L. Kavanagh: Strong polarization in the optical transmission through elliptical nanohole arrays, *Phys. Rev. Lett.* **92**(3), 37401 (2004).
11. K.J. Klein Koerkamp, S. Enoch, F.B. Segerink, N.F. van Hulst, L. Kuipers: Strong influence of hole shape on extraordinary transmission through periodic arrays of subwavelength holes, *Phys. Rev. Lett.* **92**(18), 183901 (2004).
12. J. Gómez-Rivas, C. Schotsch, P. Haring Bolivar, H. Kurz: Enhanced transmission of THz radiation through subwavelength holes, *Phys. Rev. B* **68**(20), 201306 (2003).
13. M. Beruete, M. Sorolla, M. Campillo, J.S. Dolado, L. Martín-Moreno, J. Bravo-Abad, F.J. García-Vidal: Enhanced millimeter-wave transmission through subwavelength hole arrays, *Opt. Lett.* **29**(21), 2500–2502 (2004).
14. H.J. Lezec, A. Degiron, E. Devaux, R.A. Linke, L. Martín-Moreno, F.J. García-Vidal, T.W. Ebbesen: Beaming light from a subwavelength aperture, *Science* **297**(5582), 820–822 (2002).
15. L. Martín-Moreno, F.J. García-Vidal: Optical transmission through circular hole arrays in optically thick metal films, *Opt. Express* **12**(16), 3619–3628 (2004).
16. J.D. Jackson: *Classical Electrodynamics*, 2nd ed. (Wiley, New York, 1975).
17. P.M. Morse, H. Feshbach: *Methods of Theoretical Physics* (McGraw-Hill, New York, 1953).
18. Q. Cao, P. Lalanne: Negative role of surface plasmons in the transmission of metallic gratings with very narrow slits, *Phys. Rev. Lett.* **88**(5), 57403 (2002).
19. J.B. Pendry, L. Martín-Moreno, F.J. García-Vidal: Mimicking surface plasmons with structured surfaces, *Science* **305**(5685), 847–848 (2004).
20. E. Moreno, F.J. García-Vidal, L. Martín-Moreno: Enhanced transmission and beaming of light via photonic crystal surface modes, *Phys. Rev. B* **69**(12), 121402 (2004).
21. J.A. Porto, F.J. García-Vidal, J.B. Pendry: Transmission resonances on metallic gratings with very narrow slits, *Phys. Rev. Lett.* **83**(14), 2845–2848 (1999).
22. F.J. García-Vidal, H.J. Lezec, T.W. Ebbesen, L. Martín-Moreno: Multiple paths to enhance optical transmission through a single subwavelength slit, *Phys. Rev. Lett.* **90**(21), 213901 (2003).
23. L. Martín-Moreno, F.J. García-Vidal, H.J. Lezec, A. Degiron, T.W. Ebbesen: Theory of highly directional emission from a single aperture surrounded by surface corrugations, *Phys. Rev. Lett.* **90**(16), 167401 (2003).

CHAPTER FOUR

DEVELOPMENT AND NEAR-FIELD CHARACTERIZATION OF SURFACE PLASMON WAVEGUIDES

J.-C. WEEBER¹, A.-L. BAUDRION¹, M. U. GONZÁLEZ¹, A. DEREUX¹, RASHID ZIA², AND MARK L. BRONGERSMA²

¹Laboratoire de Physique de l'Université de Bourgogne, 9 Avenue A. Savary, BP 47870, F-21078 Dijon, France, jcweeber@u-bourgogne.fr

²Geballe Laboratory for Advanced Materials, Stanford University, Stanford, CA 94305

4.1. INTRODUCTION

A polariton is an electromagnetic mode related to the oscillation of polarization charge density. At the interface between two media with frequency dependent complex dielectric functions ε_1 and ε_2 , surface polaritons with electromagnetic field exponentially decaying into both media may occur according to the well-known dispersion relation¹: $k_{sp} = (\omega/c)\sqrt{(\varepsilon_1\varepsilon_2)/(\varepsilon_1 + \varepsilon_2)}$ (where k_{sp} , ω and c are respectively the in-plane wave-vector of the surface polariton, the angular frequency and the speed of light) provided the real part of the dielectric functions in the two media are of opposite sign. If the material with the negative real part dielectric function is a metal, the polarization charge density oscillation corresponds to the oscillation of the electron gas, and then the surface polariton is called a surface plasmon polariton (SPP). Unlike SPP excited on extended metal thin films, which have been studied for decades, SPP sustained by thin metal films of finite width (metal strips) have been considered only recently. These metal strips, that can be viewed as SPP waveguides, could play an important role in the development of surface wave based optical devices.

When embedded inside a dielectric medium, thin metal strips (MS) can support long-range type SPP modes with propagation distances of a few millimeters at telecommunication frequencies.^{2–4} Based on these MS, passive and active devices such as couplers and modulators have been recently demonstrated.^{5–7} If the metal strips are deposited onto a substrate with a refractive index different from that of the superstrate, the field of the SPP penetrates more deeply into the metal, leading